Secondary Frequency and Voltage Control in Microgrids with dVOC-Based Inverters

T. Roberts and A. D. Domínguez-García
Department of Electrical and Computer Engineering
University of Illinois at Urbana-Champaign
Email: {tgr2, aledan}@illinois.edu

***Abstract*—In this paper, we address the problem of frequency and voltage control in microgrids in which generators and loads are interfaced via grid-forming (GFM) inverters. In our setting, the output voltage and frequency of the inverters is determined by a primary control scheme realized through a control strategy referred to as dispatchable virtual oscillator control (dVOC). This type of GFM primary control is known to stabilize system frequency and voltage magnitudes, but it is not capable of regulating them to their nominal values. To address this issue, we propose secondary frequency and voltage control schemes, both of which rely on integral control. The secondary frequency control scheme is centralized and similar in nature to that utilized in bulk power systems, whereas the secondary voltage control is completely decentralized. The operation of the proposed secondary frequency and voltage controls is illustrated via numerical simulations.**

***Index Terms*—Grid Forming Inverter, Dispatchable Virtual Oscillator Control, Frequency Control, Voltage Control**

I. Introduction

A microgrid can be defined as a collection of distributed energy resources (DERs) and loads interconnected via a network whose footprint is geographically small [1]. A microgrid can operate connected to a larger system in what is referred to as grid-connected mode, or can be operated without any connections to other systems in what is referred to as grid-islanded mode. When in grid-connected mode, a microgrid can be viewed as a single entity in the sense that the response of the DERs within its boundaries can be controlled and coordinated so that they collectively provide ancillary services, e.g., frequency regulation, to the external grid. When in grid-islanded mode, the DERs within the microgrid must be controlled so that they provide the power demanded by the loads while ensuring frequency and voltage stability.

In this paper, we consider AC microgrids operating in islanded mode, where generators and loads are interfaced via grid-forming (GFM) inverters. Prevalence of GFM inverters leaves the microgrid with no inertial response capability, which could potentially jeopardize frequency and voltage stability. In order to address this issue, GFM inverters are endowed with a primary control scheme, which is mainly based on (i) droop control [2], (ii) virtual synchronous machine control [3], (iii) or dispatchable virtual oscillator control (dVOC) [4], [5].

This work was supported in part by the U.S. DOE's Office of Energy Efficiency and Renewable Energy under Agreement Number EE0009025.

The settings we focus on involve microgrids whose generating- and load-type resources are interfaced with dVOC-based GFM inverters. Such dVOC-based primary control has shown to have a better dynamic performance than that of droop control [6], [7]. However, while capable of stabilizing frequency and voltage, dVOC-based primary control cannot regulate either of these to their nominal values. Our main contribution is to address this issue and propose an integral-based secondary control scheme for regulating frequency and voltage in microgrids with dVOC-based inverters.

In order to develop our secondary control scheme, we must first formulate a dynamic model describing the behavior of the microgrid under dVOC-based primary control. To do so, we assume that the dVOC-based scheme is implemented in discrete time and formulate a nonlinear state-space model describing the evolution of the magnitude and phase angles of the microgrid bus voltages. We then use this model to obtain a set of nonlinear algebraic equations describing the system steady-state behavior. These equations are essentially equivalent to a power flow model, but differ from the standard power flow model due to the presence of nonlinear dVOC-based inverters. This power flow-like model is useful because it reveals the mechanisms that cause deviations from the nominal value of frequency and bus voltage magnitudes, similar to the deviations caused by conventional droop-based primary control. The insights gained from this analysis are then used to design secondary frequency and voltage control schemes. The frequency control scheme we develop is centralized and akin to that utilized in bulk power systems, whereas the secondary voltage control is completely decentralized.

Previous work on designing secondary controllers for inverter-based microgrids has been focused on systems with droop-based inverters [8]–[12], with a few recent papers on Andronov-Hopf oscillator (AHO) based inverters [13] and virtual oscillator controlled (VOC) inverters [7]. For example, [8] proposes the use of modified droop control with a combined primary and secondary PID controller to regulate frequency, and PD controller to regulate voltage. The authors of [9] use a distributed secondary integral controller along with droop-based primary control to regulate frequency. Whereas, [10] and [11] use a ratio-consensus algorithm to adjust active power setpoints of inverter-based resources and implement frequency regulation in a droop-based system. The authors of [12] imple-

ment a secondary PI controller to regulate voltage at the point of common coupling of a microgrid, with droop-based primary control. The authors of [13] use AHO based primary control (the oscillator on which dVOC relies [6]), with an average consensus protocol for secondary control, to improve power sharing. Finally, [7] implements VOC primary control and PI secondary control on resistive networks to implement voltage and frequency control by changing oscillator parameters.

II. Microgrid Dynamics with dVOC-Based Inverters

Consider a three-phase microgrid comprising n buses indexed by the elements in $\mathcal{V} = \{1, 2, \dots, n\}$ and assume the following hold:

- **A1** The microgrid is balanced and operating in sinusoidal regime.
- **A2** There is at most one transmission line connecting each pair of buses.
- **A3** Each transmission line is short and lossless.
- **A4** Connected to each bus there is either a generating- or a load-type resource interfaced via a voltage source inverter. [This assumption can be easily extended to include grid-feeding inverters and constant power loads.]
- **A5** The reactance of each voltage source inverter output filter is small when compared to the reactance values of the network transmission lines.

Let $p_i(t)$ and $q_i(t)$ respectively denote the active and reactive power injected into bus i of the microgrid at time t. Similarly, let $V_i(t)$ and $\theta_i(t)$ respectively denote the magnitude and phase angle of the phasor associated with bus i's voltage at time t (measured relatively to a reference frame rotating at ω_0 rad/s corresponding to the microgrid's nominal frequency). Then, since Assumptions A1 – A3 hold, we have that

$$\begin{aligned} p_i(t) &= \sum_{j=1}^{n} \frac{V_i(t)V_j(t)}{X_{ij}} \sin\big(\theta_i(t) - \theta_j(t)\big), \\ q_i(t) &= -\left(B_{ii}V_i^2(t) + \sum_{\substack{j=1 \\ j\neq i}}^{n} \frac{V_i(t)V_j(t)}{X_{ij}} \cos\big(\theta_i(t) - \theta_j(t)\big) \right), \end{aligned} \tag{1}$$

where $X_{ij} > 0$ denotes the series reactance of the transmission line connecting buses i and j and $B_{ii} = -\sum_{j=1}^{n} \frac{1}{X_{ij}}$.

A. Primary Frequency and Voltage Control

As stated in Assumption A4, connected to each bus i there is either a controllable generation-type resource or an uncontrollable load-type resource interfaced with the microgrid network via a voltage source inverter. The lower-level controls of such an inverter attempt to synthesize a sinusoidal voltage at the inverter output filter capacitor terminals (see e.g., [14] for details). Then, we can describe the terminal behavior of the inverter and the resource (generating- or load-type) associated with it as a controllable voltage source, whose voltage at time t, which we denote by $e_i(t)$, is given by

$$e_i(t) = \sqrt{2}E_i(t)\sin\big(\omega_0 t + \delta_i(t)\big), \tag{2}$$

connected in series with a reactance associated with the inverter output filter [15]. As stated in Assumption A5, the value of this reactance is typically much smaller than the microgrid transmission line reactance value; therefore, we will neglect it. Thus, at time t we can approximate $V_i(t)$ and $\theta_i(t)$, by the magnitude and phase angle of $e_i(t)$ [15], i.e., $V_i(t) \approx E_i(t)$ and $\theta_i(t) \approx \delta_i(t)$ for $i = 1, 2, \dots, n$.

The values of $E_i(t)$ and $\delta_i(t)$ are essentially the reference commands passed to the lower-level inverter controls. Here we will consider the case when these are adjusted via dVOC (see, e.g., [14] for details) implemented in discrete time. Then, since $V_i(t) \approx E_i(t)$ and $\theta_i(t) \approx \delta_i(t)$, the evolution of $\theta_i(t)$ and $V_i(t)$ is governed by the same update rule associated with the discrete-time dVOC. For some $T \geq 0$ and $k = 0, 1, \dots$, define $\theta_{i,k} := \theta_i(kT)$, $V_{i,k} := V_i(kT)$, $p_{i,k} := p_i(kT)$ and $q_{i,k} := q_i(kT)$. Then, we have that

$$\begin{aligned} \theta_{i,k+1} &= \theta_{i,k} + \frac{Ta_i}{V_{i,k}^2}(p_{i,k}^{\circ} - p_{i,k}), \\ V_{i,k+1} &= V_{i,k} + d_i T\Big((V_i^{\circ})^2 - V_{i,k}^2\Big)V_{i,k} + \frac{a_i T}{V_{i,k}}(q_{i,k}^{\circ} - q_{i,k}), \end{aligned} \tag{3}$$

where a_i and d_i are constants derived from the AHO circuit used to implement dVOC [6], V_i° is the nominal inverter voltage magnitude, and $p_{i,k}^{\circ}$ and $q_{i,k}^{\circ}$ are either: (i) control inputs denoted by $p_{i,k}^{r}$ and $q_{i,k}^{r}$, respectively, or (ii) extraneous disturbances denoted by $p_{i,k}^{d}$ and $q_{i,k}^{d}$, respectively. The control inputs, $p_{i,k}^{r}$ and $q_{i,k}^{r}$, can be set by a secondary control system and $p_{i,k}^{r}$ is positive for the case when there is a generating-type resource connected to bus i. The extraneous disturbances, $p_{i,k}^{d}$ and $q_{i,k}^{d}$, are uncontrollable and p_i^{d} is negative when there is a load-type resource connected to bus i.

Without loss of generality, assume that buses 1 to m have load-type resources connected to them, whereas buses $m+1$ to n have generating-type resources connected to them. Then, by using (1) together with (3), it follows that

$$\theta_{i,k+1} = \theta_{i,k} + \frac{Ta_i}{V_{i,k}^2}\left(p_{i,k}^{\circ} - \sum_{j=1}^{n} \frac{V_{i,k}V_{j,k}}{X_{ij}} \sin\big(\theta_{i,k} - \theta_{j,k}\big) \right), \tag{4}$$

$$\begin{aligned} V_{i,k+1} = V_{i,k} &+ d_i T\Big((V_i^{\circ})^2 - V_{i,k}^2\Big)V_{i,k} + \frac{a_i T}{V_{i,k}} q_{i,k}^{\circ} \\ &+ \frac{a_i T}{V_{i,k}}\left(B_{ii}V_{i,k}^2 + \sum_{\substack{j=1 \\ j\neq i}}^{n} \frac{V_{i,k}V_{j,k}}{X_{ij}} \cos\big(\theta_{i,k} - \theta_{j,k}\big) \right), \end{aligned} \tag{5}$$

where

$$p_{i,k}^{\circ} = \begin{cases} p_{i,k}^{d}, & i = 1, 2, ..., m, \\ p_{i,k}^{r}, & i = m+1, m+2, ..., n, \end{cases} \tag{6}$$

$$q_{i,k}^{\circ} = \begin{cases} q_{i,k}^{d}, & i = 1, 2, ..., m, \\ q_{i,k}^{r}, & i = m+1, m+2, ..., n, \end{cases} \tag{7}$$

with $p_i^{r} > 0$ and $p_i^{d} < 0$.

B. Steady-State Operating Point

For the model in (4) – (5) and (6) – (7), assume that $p^d_{i,k} = p^d_i$, $p^r_{i,k} = p^r_i$, $q^d_{i,k} = q^d_i$, and $q^r_{i,k} = q^r_i$, where p^d_i, p^r_i, q^d_i, and q^r_i are constants. Then, we can compute the steady-state operating point as follows. First note that in steady-state, we have that $\theta_{i,k+1} - \theta_{i,k} = \mu,\ i = 1, 2, \ldots, n$, where μ is some constant, and $V_{i,k+1} = V_{i,k} = V_i$; thus, $\theta_{i,k} - \theta_{j,k} = \theta_{ij}$ for all $i \neq j$. Then, it follows from (4) that

$$\mu = \frac{T\Big(\sum_{\ell=1}^{m} p^d_\ell + \sum_{\ell=m+1}^{n} p^r_\ell\Big)}{\sum_{\ell=1}^{n} V_\ell^2/a_\ell}. \tag{8}$$

Then, by noting (2) (recall that $\delta_i(t) \approx \theta_i(t)$) and the expression for μ in (8), we can conclude that in steady state, the voltage synthesized by each inverter will have a frequency $\omega_0 + \overline{\omega}$, where

$$\overline{\omega} = \mu/T. \tag{9}$$

Thus, in steady state, we have that $V_i,\ i = 1, 2, \ldots, n$ and $\theta_{ij},\ i \neq j$, must satisfy the following relations:

$$\begin{aligned} 0 = &- V_i^2/a_i \underbrace{\frac{\Big(\sum_{\ell=1}^{m} p^d_\ell + \sum_{\ell=m+1}^{n} p^r_\ell\Big)}{\sum_{\ell=1}^{n} V_\ell^2/a_\ell}}_{=\overline{\omega}} \\ &+ \left(p^\circ_i - \sum_{j=1}^{n} \frac{V_i V_j}{X_{ij}} \sin\big(\theta_{ij}\big)\right), \end{aligned} \tag{10}$$

$$\begin{aligned} 0 = {} & d_i\Big((V^\circ_i)^2 - V_i^2\Big)V_i + \frac{a_i}{V_i} q^\circ_i \\ &+ \frac{a_i}{V_i}\left(B_{ii}V_i^2 + \sum_{\substack{j=1 \\ j\neq i}}^{n} \frac{V_i V_{jk}}{X_{ij}} \cos\big(\theta_{ij}\big)\right); \end{aligned} \tag{11}$$

this is essentially the power flow model for a microgrid with dVOC-based inverters. Note that in (10) – (11) there are $2n - 1$ unknowns, namely, $V_i\ i = 1, 2, \ldots, n$, and $\theta_{ij},\ i = 1, 2, \ldots, n,\ j > i$, and although there are $2n$ equations, only $2n - 1$ are independent (among the first n equations, only $n - 1$ are independent).

III. Closed-Loop Frequency and Voltage Control

While dVOC-based inverters are able to stabilize frequency and voltage, they will not ensure proper regulation of system frequency and bus voltage. In particular, we have shown that, unless $\sum_{\ell=1}^{m} p^d_\ell + \sum_{\ell=m+1}^{n} p^r_\ell = 0$, system frequency will settle to $\omega_0 + \overline{\omega}$, with $\overline{\omega}$ as given in (9). Also, by examining (10) – (11) it is not clear a priori what the values of the steady-state bus voltage magnitudes will be, i.e., there is no guarantee that bus voltage magnitudes will be properly regulated. To address these issues we will design secondary frequency and voltage control systems.

A. Secondary Frequency Control

In light of the steady-state relation in (9), one can see that by regulating the $p^r_{i,k}$'s so that their sum tracks the negative of the sum of the $p^d_{i,k}$'s, the system frequency can be regulated to its nominal value. This can be accomplished via feedback control as follows. First, let $\omega_{i,k} = (\theta_{i,k+1} - \theta_{i,k})/T,\ i = 1, 2, \ldots, n$, and define the *weighted average frequency error* at instant k as follows

$$\begin{aligned} \overline{\omega}_k &:= \frac{\sum_{i=1}^{n} \omega_{i,k} V_{i,k}^2/a_i}{\sum_{i=1}^{n} V_{i,k}^2/a_i} \\ &= \frac{1}{\sum_{i=1}^{n} V_{i,k}^2/a_i}\left(\sum_{i=1}^{m} p^d_{i,k} + \sum_{i=m+1}^{n} p^r_{i,k}\right), \end{aligned} \tag{12}$$

where the last equality follows from (4) after slightly rearranging the equations and summing them up over i. The $p^r_{i,k}$'s are then regulated via discrete-time integral control as follows:

$$\begin{aligned} y_{k+1} &= y_k + \alpha\overline{\omega}_k, \\ p^r_{i,k} &= p^*_i + \beta_i y_k, \end{aligned} \tag{13}$$

where p^*_i is constant (it can be set, e.g., by optimization-based tertiary control), and so are the controller gains α and β_i. Here the β_i's determine how the steady-state value of y_k is apportioned among the different generators, i.e., it determines power-sharing.

Notice that in (13) we have used a single integrator instead of using a local integrator with local frequency error, i.e., $\overline{\omega}_{i,k} := (\theta_{i,k+1} - \theta_{i,k})/T$, as a feedback signal to regulate $p^r_{i,k}$. While local integrators might look appealing due to the fact that the resulting control scheme is completely decentralized, it can be shown that such decentralized scheme would not yield proper power apportioning among the generators and could result in stability issues if the measurements used by the local controllers are biased or corrupted by noise. In fact, it is well-known in the power system and control literature that the use of such decentralized controls is problematic [16]–[18].

B. Secondary Voltage Control

Inspection of (11) reveals that, for small θ_{ij}'s (typically the case under normal operating conditions), there is a strong coupling between the V_i's and the q°_i's. Then, if we assume that changes in the $q^d_{i,k}$ are relatively small as compared to changes in the $p^d_{i,k}$, regulating the $q^r_{i,k}$'s will provide with a mechanism to regulate the $V_{i,k}$'s. We implement such regulation mechanism via feedback control as follows. First, define the *voltage deviation* at bus i as follows:

$$\Delta V_{i,k} = V^*_i - V_{i,k}, \tag{14}$$

where V^*_i is a constant that can be set by a tertiary control. Then, the $q^r_{i,k}$'s are regulated using discrete-time local controllers as follows:

$$\begin{aligned} z_{i,k+1} &= z_{i,k} + \kappa_i \Delta V_{i,k}, \\ q^r_{i,k} &= q^*_i + \gamma_i z_{i,k}, \end{aligned} \tag{15}$$

where q^*_i is constant (it can be set, e.g., by optimization-based tertiary control), and so are the controller gains κ_i and γ_i.

Notice that the scheme above will ensure that $V_{i,k}$ is driven to V^*_i for $i = m + 1, m + 2, \ldots, n$, i.e., only generator bus voltages are regulated directly by the local voltage controllers.

However, since changes in the $p^{\circ}_{i,k}$'s mostly affect frequency and we have assumed that the changes in $q^{d}_{i,k}$ are relatively small, the proposed mechanism is effective at maintaining load bus voltages close to their nominal value. Also note that if deviations in the $q^{d}_{i,k}$ are large enough so that the $\Delta V_{i,k}$'s for load buses become unacceptable, tertiary control could be executed so that new values for V_i^*'s and q_i^*'s are chosen that result in acceptable $\Delta V_{i,k}$'s at all buses.

IV. Simulation Results

We will illustrate the performance of our proposed secondary controller on the three-bus microgrid shown in Fig. 1, which has a load-type resource connected to bus 1 and generating-type resources connected to buses 2 and 3. As previously stated, all three resources are interfaced via dVOC-based GFM inverters.

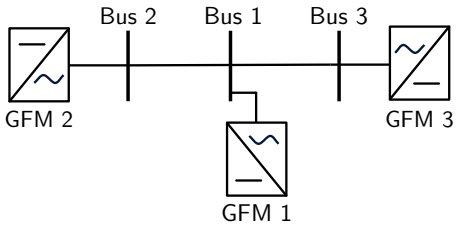

Fig. 1: Three-phase microgrid, wherein bus 1 is a load bus and buses 2 and 3 are generation buses.

The microgrid closed-loop dynamic behavior is described by (4) – (5), (13), and (15) with $n = 3$ and $m = 1$. We assume all inverters are identical, i.e., $a_1 = a_2 = a_3 = a$, $d_1 = d_2 = d_3 = d$, and $V_1^{\circ} = V_2^{\circ} = V_3^{\circ} = V^{\circ}$. The parameter values and initial conditions used to populate this model are provided in Table I. All variables and parameters are in per-unit unless otherwise specified.

The simulation for primary-control is executed for 200 s, with load changes every 20 s, as shown in Fig. 2. Figure 3a illustrates that while frequency is stabilized post-disturbance, it settles to a new value away from nominal after every perturbation; bus voltage magnitudes behave similarly as shown in Fig. 3b. This illustrates that while dVOC-based primary control is adept at stabilizing both frequency and voltage, secondary control is necessary to return values to nominal.

The simulation for closed-loop secondary control also uses the load profiles shown in Fig. 2. Parameters and initial conditions for the closed-loop simulation are provided in Table II, with all others matching those in Table I. As seen in Fig. 4a, the developed secondary frequency control drives frequency mismatch, $\overline{\omega}$ back to nominal after every load change. Figure 4b depicts a similar phenomenon, wherein voltage magnitudes at generation-type resources, V_2, V_3, are driven back to nominal after disturbances occur. Whereas, the voltage at the uncontrollable load, V_1, is lower than the nominal value, which is expected since the voltage at this bus is not directly regulated by the secondary voltage control.

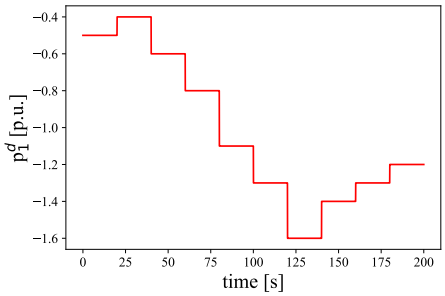

(a) Active power load profile for bus 1.

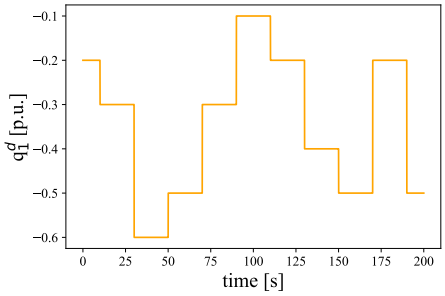

(b) Reactive power load profile for bus 1.

Fig. 2: Active and reactive power load profiles.

V. Concluding Remarks

Previous inverter-based microgrid systems have mostly relied on droop-based primary control for frequency and voltage regulation, with various secondary control techniques. This paper examines dVOC-based primary control with secondary integral control for both frequency and voltage. Simulation results illustrate that after load disturbances in the system, dVOC-based primary control is able to stabilize frequency and voltage deviations, and secondary control is able to return both frequency and voltage to nominal values.

References

[1] D. T. Ton and M. A. Smith, "The U.S. Department of Energy's Microgrid Initiative," *The Electricity Journal*, vol. 25, Issue 8, 2012, pp. 84-94.

[2] M. C. Chandorkar, D. M. Divan, and R. Adapa, "Control of parallel connected inverters in standalone AC supply systems," *IEEE Trans. Ind. Appl.*, vol. 29, no. 1, pp. 136–143, Jan. 1993.

[3] Q.-C. Zhong and G. Weiss, "Synchronverters: Inverters that mimic synchronous generators," *IEEE Trans. Ind. Electron.*, vol. 58, no. 4, pp. 1259–1267, Apr. 2011.

[4] M. Lu, S. Dutta, V. Purba, S. Dhople, and B. Johnson, "A grid-compatible virtual oscillator controller: Analysis and design," IEEE Energy Conversion Congress and Exposition, 2019, pp. 2643–2649

[5] M. Colombino, D. Groß, J. Brouillon, and F. Dörfler, "Global phase and magnitude synchronization of coupled oscillators with application to the control of grid-forming power inverters," *IEEE Trans. Autom. Control*, vol. 64, no. 11, pp. 4496–4511, Nov. 2019.

[6] M. Lu, V. Purba, S. Dhople and B. Johnson, "Comparison of Droop Control and Virtual Oscillator Control Realized by Andronov-Hopf Dynamics," in Proc. of the IEEE Industrial Electronics Society, 2020, pp. 4051-4056.

[7] M. A. Awal, H. Yu, H. Tu, S. M. Lukic and I. Husain, "Hierarchical Control for Virtual Oscillator Based Grid-Connected and Islanded Microgrids," in IEEE Transactions on Power Electronics, vol. 35, no. 1, pp. 988-1001, Jan. 2020.

TABLE I: Primary Control System Parameters.

Parameter	a	d	V°	T	x_1	x_2	p_1^d	p_2^r	p_3^r	q_1^d	q_2^r	q_3^r
Value	0.165	2.285	1.0	0.001	1.0	1.0	-0.5	0.2	0.3	-0.2	0.05	0.15

Initial Conditions	$\overline{\omega}$	θ_1	θ_2	θ_3	V_1	V_2	V_3
Value	0.0	0.0	0.2030	0.3065	0.9909	1.000	1.003

TABLE II: Secondary Control System Parameters.

Parameter	p_1^d	p_2^*, p_3^*	q_1^d	q_2^*, q_3^*	V^*	α	β_2, β_3	κ_2, κ_3	γ_2, γ_3
Value	-0.5	0.25	-0.2	0.1	1.0	-90.0	0.5	50	1.5

Initial Conditions	$\overline{\omega}$	θ_1	θ_2	θ_3	V_1	V_2	V_3	y	z_2	z_3
Value	0.0	0.0	0.2032	0.3076	0.9908	1.0	1.0	0.0	-0.0136	-0.0628

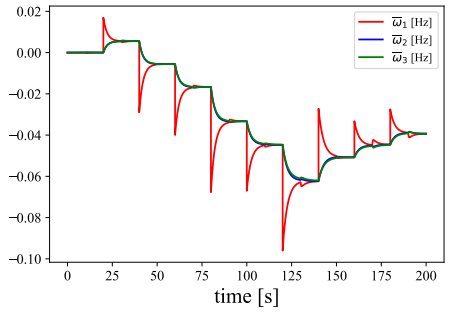

(a) Frequency mismatch, $\overline{\omega}_i$, $i = 1, 2, 3$.

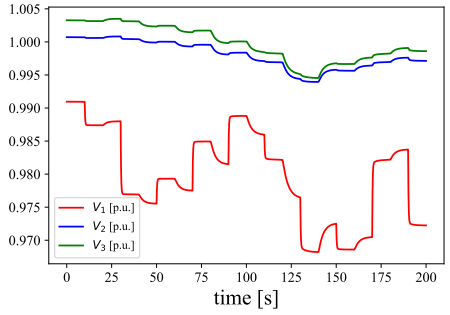

(b) Voltage magnitude, V_i, $i = 1, 2, 3$.

Fig. 3: dVOC-based primary control simulation results.

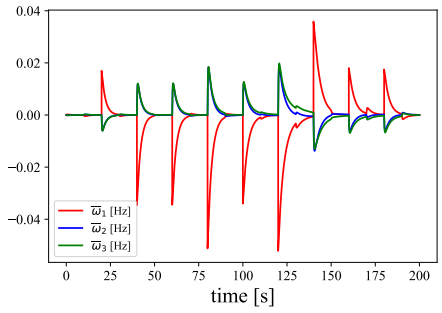

(a) Frequency mismatch, $\overline{\omega}_i$, $i = 1, 2, 3$.

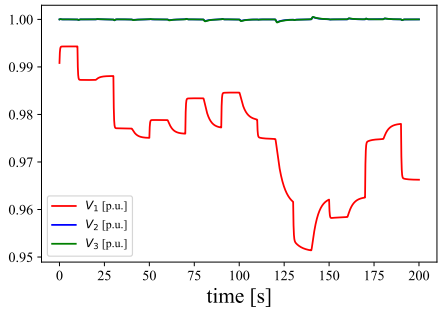

(b) Voltage magnitude, V_i, $i = 1, 2, 3$.

Fig. 4: Closed loop secondary control simulation results.

[8] J. M. Guerrero, L. G. de Vicuna, J. Matas, M. Castilla and J. Miret, "A wireless controller to enhance dynamic performance of parallel inverters in distributed generation systems," *IEEE Transactions on Power Electronics*, vol. 19, no. 5, pp. 1205-1213, Sept. 2004.

[9] J. W. Simpson-Porco, F. Dörfler, F. Bullo, Q. Shafiee and J. M. Guerrero, "Stability, power sharing, and distributed secondary control in droop-controlled microgrids," in Proc. of IEEE International Conference on Smart Grid Communications, 2013.

[10] S. T. Cady, A. D. Domínguez-García and C. N. Hadjicostis, "A Distributed Generation Control Architecture for Islanded AC Microgrids," *IEEE Transactions on Control Systems Technology*, vol. 23, no. 5, pp. 1717-1735, Sept. 2015.

[11] S. Nigam, O. Ajala, M. Zholbaryssov, A. D. Domínguez-García and P. W. Sauer, "Distributed Secondary Frequency Control in AC Microgrids with Lossy Electrical Networks," in Proc. of the IEEE Power and Energy Society General Meeting, 2020.

[12] M. Savaghebi, A. Jalilian, J. C. Vasquez and J. M. Guerrero, "Secondary Control Scheme for Voltage Unbalance Compensation in an Islanded Droop-Controlled Microgrid," *IEEE Transactions on Smart Grid*, vol. 3, no. 2, pp. 797-807, June 2012.

[13] I. Sowa, T. T. Tran, T. Heins, D. Raisz and A. Monti, "An Average Consensus Algorithm for Seamless Synchronization of Andronov-Hopf Oscillator Based Multi-Bus Microgrids," in IEEE Access, vol. 9, pp. 90441-90454, 2021.

[14] O. Ajala, M. Lu, S. Dhople, B. B. Johnson and A. Dominguez-Garcia, "Model Reduction for Inverters with Current Limiting and Dispatchable Virtual Oscillator Control," *IEEE Transactions on Energy Conversion*.

[15] A. D. Domínguez-García, *Large-Scale System Analysis Under Uncertainty with Electric Power Applications*, Cambridge Univ. Press, 2022.

[16] M. Andreasson, D. V. Dimarogonas, H. Sandberg and K. H. Johansson, "Distributed PI-control with applications to power systems frequency control," in Proc. of American Control Conference, 2014.

[17] F. Dörfler and S. Grammatico, "Gather-and-broadcast frequency control in power systems," *Automatica*, vol. 79, pp. 296-305, 2017.

[18] K. J. Aström and T. Hägglund, *Advanced PID Control*, The Instrumentation Systems and Automation Society, 2006.